IEEE Access
Multidisciplinary | Rapid Review | Open Access Journal

Received 15 July 2023, accepted 1 August 2023, date of publication 4 August 2023, date of current version 14 August 2023.

Digital Object Identifier 10.1109/ACCESS.2023.3302255

RESEARCH ARTICLE

Analysis of Rotation Magnetized Direction Permanent Magnet Thrust Bearing for Maximum Characteristics Using a Complete Generalized Optimization Procedure and a Computational Framework

SUPREETH D. K.[1], SIDDAPPA I. BEKINAL[1], SHIVAMURTHY R. C.[1], VIJAY G. S.[1], AND MRITYUNJAY DODDAMANI[2]

[1]Department of Mechanical and Industrial Engineering, Manipal Institute of Technology, Manipal Academy of Higher Education (MAHE), Manipal 576104, India
[2]School of Mechanical and Materials Engineering, Indian Institute of Technology Mandi, Mandi, Himachal Pradesh 175075, India

Corresponding authors: Siddappa I. Bekinal (siddappa.bekinal@manipal.edu) and Shivamurthy R. C. (shivamurthy.rc@manipal.edu)

This work was supported in part by the Aeronautics Research and Development Board, Defence Research and Development Organisation (DRDO), Delhi, for supporting the envisaged research vide under Grant ARDB/01/1072037/M/I; and in part by the Manipal Institute of Technology, Manipal Academy of Higher Education, Manipal, for carrying out the research work.

ABSTRACT This article presents the generalized optimal design procedure and MATLAB app for rotation magnetized direction (RMD) permanent magnet thrust bearing for maximum characteristics based on air gap, outer diameter, and length of a bearing concerning the available space for replacing conventional bearings in industrial applications. To begin with, MATLAB codes for solving the three-dimensional (3D) equations of force and stiffness are developed. Then, the curve fit correlations are established to obtain the optimized design parameters for maximum bearing characteristics. The optimization process is further extended for different aspect ratios and airgap values of the bearing using the curve fit equations of design variables. The proposed pragmatic and generalized optimization procedure is demonstrated using the application examples. Finally, to overcome the process of solving the complex design equations and usage of optimization methods, Industry ready MATLAB app is developed for designing and optimizing the RMD thrust bearing based on only three general parameters (g, D4, and L). The usage of the proposed computational framework in the industry is demonstrated by discussing the case study from the literature.

INDEX TERMS Curve fitting, MATLAB app, optimization, rotation magnetized direction, thrust bearing.

ABBREVIATION

AMB	Active magnetic bearing.
3D	Three-dimensional.
a	Number of stator rings.
Br	Magnetic flux density.
c	Discrete elements on the faces of the magnet rings.
D1	Inside diameter of the rotor ring.
D2	Outside diameter of the rotor ring .
D3	Inside diameter of the stator ring .
D4	Outside diameter of the stator ring .
e	Number of rotor rings .
f	Polarized faces of the stator.
FEA	Finite element analysis.
F_{zmax}	Maximum axial force.
g	Air gap.
h	The axial thickness of rings .
j	Number of surface elements on the faces of the rotor.
K_{zmax}	Maximum axial stiffness.
y	Polarized faces of the rotor .

The associate editor coordinating the review of this manuscript and approving it for publication was Su Yan.

This work is licensed under a Creative Commons Attribution-NonCommercial-NoDerivatives 4.0 License.
For more information, see https://creativecommons.org/licenses/by-nc-nd/4.0/

I. INTRODUCTION

Non-contact bearings are well suited for supporting the rotating objects in high-speed machinery. Conventional bearings could serve the purpose, but they require lubrication, maintenance, and are prone to wear and tear. Hence with electromagnetic forces, rotating objects can be supported without any mechanical contact because they are friction-free, and can operate at much higher speeds than conventional bearings [1]. Electromagnetic forces can be generated with help of permanent magnets or electromagnets. A permanent magnet bearing (PMB) uses permanent magnets to support the rotor with the help of attractive and repulsive forces exerted by magnets fitted to the rotor and stator. An active magnetic bearing (AMB) requires input energy, sensors, and electrical and electronic components, while a PMB doesn't. Due to their attractive features, PMB have been used to support low [2], [3], and high-speed [4], [5], [6], [7] applications. Despite their attractive features, PMB suffers from instability and poor damping [8]. With help of AMB [9] or superconducting bearings [10], or mechanical bearings [11] the stability of the rotor supported by PMB could be improved. Whereas the damping can be enhanced either with a viscoelastic damper [12] or eddy current dampers [13], [14]. Mathematical equations were developed to ascertain force and stiffness for single [15], [16], [17] and multi-ring radial [18], [19], [20], [21], [22] and thrust PMB [23], [24], [25], [26]. Optimization of PMB for their geometrical characteristics is necessary to obtain bearing characteristics as comparable to conventional bearings. In [27] and [28], a single objective function was utilized to optimize monolithic PMB in a particular volume for maximum characteristics. In stack-structured permanent magnet (PM) bearings where rings can be axially/radially or perpendicularly polarized, authors in [29] and [30] performed optimization within a particular cylindrical volume. Generalized plots for optimized parameters were provided concerning the outer diameter of the bearing. In our earlier research efforts, a generalized optimum design methodology [31] for axially magnetized multi-ring PM radial and thrust bearings was presented by utilizing 3D mathematical equations of force and stiffness. In addition, a handy MATLAB computational framework [32] suitable for design and optimization based on three parameters (g, D4, and L) concerning control volume was presented. Designers could directly use the presented framework in the industry for obtaining the optimal design variables for maximum bearing characteristics without solving complicated 3D equations and using optimization techniques.

As it was shown in the literature [30] the RMD configuration is much superior to the conventional one in terms of force and stiffness. Optimization of the RMD configuration is carried out concerning to aspect ratio (L/D4) as shown in Fig. 1. The parameters (n, D1, D2 and D4) are optimized for maximum bearing characteristics. After optimization, the designer has to solve complicated equations of bearing features for its usage in the industry. To overcome this, a pragmatic optimization, and the generalization of the same with respect to any aspect ratio is presented in this paper. In addition, A MATLAB app suitable for the design and optimization of RMD thrust-bearing configuration for any aspect ratio and magnetic flux density (Br) is presented.

II. ROTATION MAGNETIZED DIRECTION THRUST BEARING CONFIGURATION

The force as well as stiffness generated by the single-ring PMB, are very less as compared to the conventional bearing [8]. This problem can be solved by incorporating multiple rings into the stator and rotor to form a stacked structure where rings are magnetized either in the axial or radial direction. It can be further improved by employing an RMD structure where rings are magnetized axially and radially and are arranged in opposition.

Rotation magnetized direction PM thrust bearing configuration is shown in Fig. 1. The inner rings are attached to the rotor, while the outer one to the stator. The rotor will be levitated as a result of the repulsive and attractive forces between the magnet's faces.

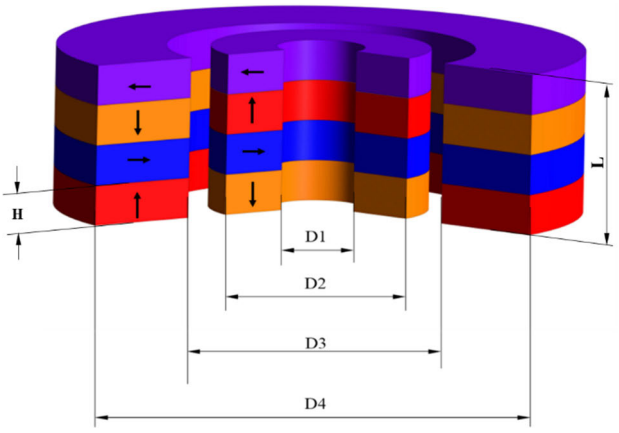

FIGURE 1. RMD thrust bearing configuration employed for optimization.

III. SEMI-ANALYTICAL MODEL

Rotation magnetized direction thrust-bearing properties are evaluated based on a mathematical model presented in this section. In RMD thrust bearings, the stator rings exert a net force on rotor rings due to the interaction between (i) Axially-Axially (ii) Radially-Radially, and (iii) Axially-Radially or Radially-Axially polarized magnet rings. The Fig. 2 depicts the magnetic interaction that occurs between the faces of ring magnets. Based on the Cartesian coordinate system, the e^{th} ring is mounted on the rotor, which can move freely relative to the a^{th} ring mounted on the stator. 1, 2, 3, and 4 are the charged surfaces of magnet rings. Based on the interactions between all faces of stator-rotor rings, the net axial force acting on the rotor rings is given by equation (1) by

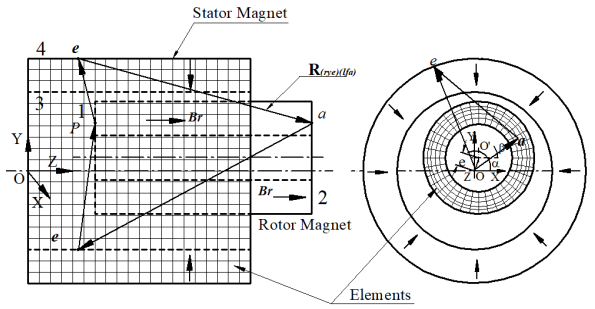

FIGURE 2. Interactions between axially and radially polarized magnet rings [26].

Bekinal et al. [26].

$$F_z = \frac{B_r^2}{4\pi\mu_0} \sum_{e=1}^{n} \sum_{a=1}^{n} \sum_{y=1}^{2} \sum_{f=3}^{4} \sum_{e=1}^{c} \sum_{j=1}^{c} \frac{S_{rye} S_{jfa}}{R^3_{(rye)(jfa)}} \boldsymbol{R}_{(rye)(lfa)} (-1)^{(y+f)} (-1)^{(b)} \quad (1)$$

Number of discrete elements on the faces of the magnet rings is c. The surface area (SA) of r^{th} element positioned on y^{th} surface of the e^{th} rotor magnet is denoted as S_{rye} and S_{jfa} denotes the SA of the j^{th} element positioned on the f^{th} surface of the a^{th} stator magnet. Where,

$$\boldsymbol{R} = \sqrt{\left(X_{jfa} - X_{rye}\right)^2 + \left(Y_{jfa} - Y_{rye}\right)^2 + \left(Z_{jfa} - Z_{rye}\right)^2}$$

and

$$R_{(rye)(jfa)} = \left(X_{jfa} - X_{rye}\right)\boldsymbol{i} + \left(Y_{jfa} - Y_{rye}\right)\boldsymbol{j} + \left(Z_{jfa} - Z_{rye}\right)\boldsymbol{k}$$

The position coordinates of the elements of the faces are given below.

If e and a are of odd values

$$\begin{aligned} X_{rye} &= (x + r_{mr}\cos\beta)\, i \\ Y_{rye} &= (y + r_{mr}\sin\beta)\, j \\ Z_{rye} &= (z{+}(e{-}1)l)\, \boldsymbol{k} \\ X_{jfa} &= (r_{ms}\cos\alpha)\, i \\ Y_{jfa} &= (r_{ms}\cos\alpha)\, \boldsymbol{j} \\ Z_{jfa} &= (al)\, \boldsymbol{k} \end{aligned} \quad (2)$$

If e and a are of even values

$$\begin{aligned} X_{rye} &= (x + R2\cos\beta)\, i \\ Y_{rye} &= (y + R2\sin\beta)\, \boldsymbol{j} \\ Z_{rye} &= (z + l_m)\, \boldsymbol{k} \\ X_{jfa} &= (R4\cos\alpha)\, i \\ Y_{jfa} &= (R4\sin\alpha)\, \boldsymbol{j} \\ Z_{jfa} &= (l_m)\, \boldsymbol{k} \\ l_m &= l\,(h-1) + (j-1)\,\frac{1}{N_1} + \frac{1}{2N_1} \end{aligned} \quad (3)$$

where h is either e or a and e and $a = 1, 2, 3, \ldots$ n, The surfaces of the polarized rings are divided into N1 number of elements and j=1, 2,3,...N1.

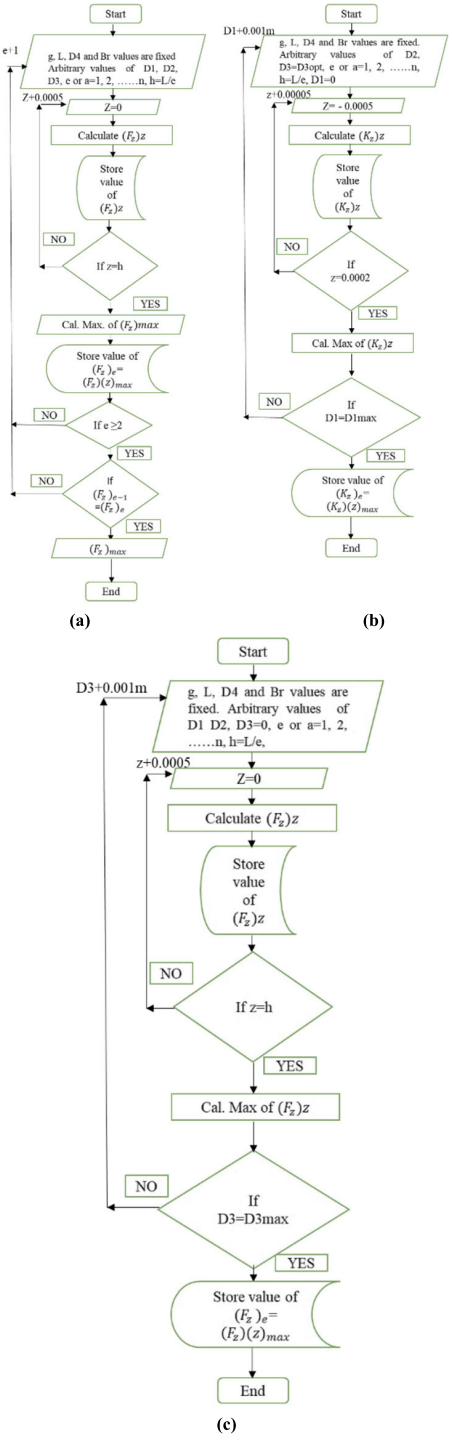

FIGURE 3. Flow charts depicting the optimization process (a) optimization of the number of rings for maximum force (b) optimization of D1 for maximum stiffness (c) optimization of D3 for maximum force.

The following criteria are used to evaluate the value of b in equation (1).

If e is even or odd and $(e{+}a)$ is even,

$$b = \left(\frac{(e+a)}{2} - e\right) \quad (4)$$

TABLE 1. Curve fit equations of RMD thrust bearing for F_{zmax}.

Sl. No.	Optimized Parameters	Curve fit equations
1.	$n_{opt} = \frac{H_o}{L}$	$\frac{H_o}{D_4} = -819 \times \left(\frac{g}{D_4}\right)^3 + 55.8 \times \left(\frac{g}{D_4}\right)^2 - 0.0957 \times \left(\frac{g}{D_4}\right) + 0.0509$
2.	D_{1opt}	$\left(\frac{D_1}{D_4}\right) = -517.2 \times \left(\frac{g}{D_4}\right)^3 + 74.11 \times \left(\frac{g}{D_4}\right)^2 - 3.326 \times \left(\frac{g}{D_4}\right) + 0.3464$
3.	D_{3opt}	$\left(\frac{D_1}{D_4}\right) = 5.956 \times 10^{-15} \times \left(\frac{g}{D_4}\right) + 0.8$
4.	D_{2opt}	$D_{2\,opt} = D_{3\,opt} - 2g$

If e is even and (e+a) is odd

$$b = \left(\frac{(e + a + 1)}{2} - e\right) \tag{5}$$

If e is odd and (e+a) is odd

$$b = \left(\frac{(e + a - 1)}{2} - e\right) \tag{6}$$

The axial stiffness produced in the RMD thrust bearing is given by Bekinal et al [26].

$$K_Z = -\frac{dF_z}{dZ} \tag{7}$$

By using MATLAB, the maximum force as well as stiffness, are determined by employing the equations (1)-(7).

IV. OPTIMIZATION OF RMD THRUST BEARING

By optimizing the design parameters, the bearing features of the RMD thrust bearing can be maximized. For a given bearing volume, the important bearing characteristics were optimized. The optimization variables are D1, D2, D3, and n, and the flowchart below (Fig. 3) illustrates the methodology used.

Based on the analysis results presented in [30] and [31], $D1$, $D2$, $D3$, and n were taken as the parameters which affect the force and stiffness of a RMD thrust bearing for a given $D4$, L and g values. Hence these variables were taken for the optimization process.

Optimization details of variables and relationships between optimum design variables (n_{opt}, $D1_{opt}$, $D2_{opt}$, and $D3_{opt}$) and the ratio (g/D4) were presented in [33]. In addition, curve fit equations (shown in Table 1 and Table 2) expressing relationships were also presented.

These curve fit equations have been utilized to ascertain the optimized parameters for the bearing having dimensions, $D_4 = 70$ mm, $g = 2$ mm, and $L = 70$ mm, the corresponding optimized dimensions for RMD thrust bearing for $\boldsymbol{F_{zmax}}$ and $\boldsymbol{K_{zmax}}$ are given in Table 3.

TABLE 2. Curve fit equations of RMD thrust bearing for K_{zmax}.

Sl. No.	Optimized Parameters	Curve fit equations
1.	$n_{opt} = \frac{H_o}{L}$	$\frac{H_o}{D_4} = -218.1 \times \left(\frac{g}{D_4}\right)^3 + 6.597 \times \left(\frac{g}{D_4}\right)^2 + 1.068 \times \left(\frac{g}{D_4}\right) + 0.01324$
2.	D_{1opt}	$\left(\frac{D_1}{D_4}\right) = -2.913 \times 10^8 \times \left(\frac{g}{D_4}\right)^6 + 4.327 \times 10^7 \times \left(\frac{g}{D_4}\right)^5 - 2.529 \times 10^6 \times \left(\frac{g}{D_4}\right)^4 + 7.37 \times 10^4 \times \left(\frac{g}{D_4}\right)^3 - 1114 \times \left(\frac{g}{D_4}\right)^2 + 8.138 \times \left(\frac{g}{D_4}\right) + 0.4281$
3.	D_{3opt}	$\left(\frac{D_1}{D_4}\right) = 4.928 \times 10^{-15} \times \left(\frac{g}{D_4}\right) + 0.825$
4.	D_{2opt}	$D_{2\,opt} = D_{3\,opt} - 2g$

TABLE 3. Optimized dimensions of RMD thrust bearing.

Optimized design variables	For F_{zmax}	For K_{zmax}
n_{opt}	13	22
D_{1opt} (mm)	21	32
D_{2opt} (mm)	52	56
D_{3opt} (mm)	56	58
D_4 (mm)	70	70
g (mm)	2	2
L (mm)	70	70
Br (T)	1.2	1.2
Bearing Features	$\boldsymbol{F_{zmax}}$ = 4880.5 N	$\boldsymbol{K_{zmax}}$=7210335.58 N mm

The maximum axial force calculated from the optimization is validated using ANSYS. The magnet rings considered for analysis are N35 grade with $\boldsymbol{B_r} = 1.2$ T, relative permeability $\boldsymbol{\mu_r} = 1.1$, and coercive force $\boldsymbol{H_c} = 868$ kA/m. Modeling of the thrust bearing is based on a Solid97 elements with dimensions calculated using equations given in Table 1. The rings are axially and radially magnetized and are arranged in opposition (Fig. 4 (a)). In Fig. 4(b), flux lines generated in thrust bearing are shown. The magnetic virtual displacement method is used to ascertain the maximum force (Fig. 4(c)) in the RMD thrust bearing. The maximum axial force generated is 5191.3 N for an axial offset of 5.5 mm which is in good agreement with force value of an optimized configuration.

V. OPTIMIZATION OF RMD CONFIGURATION CONCERNING DIFFERENT ASPECT RATIOS

The optimum design methodology for RMD thrust bearing for different aspect ratios has been presented in this

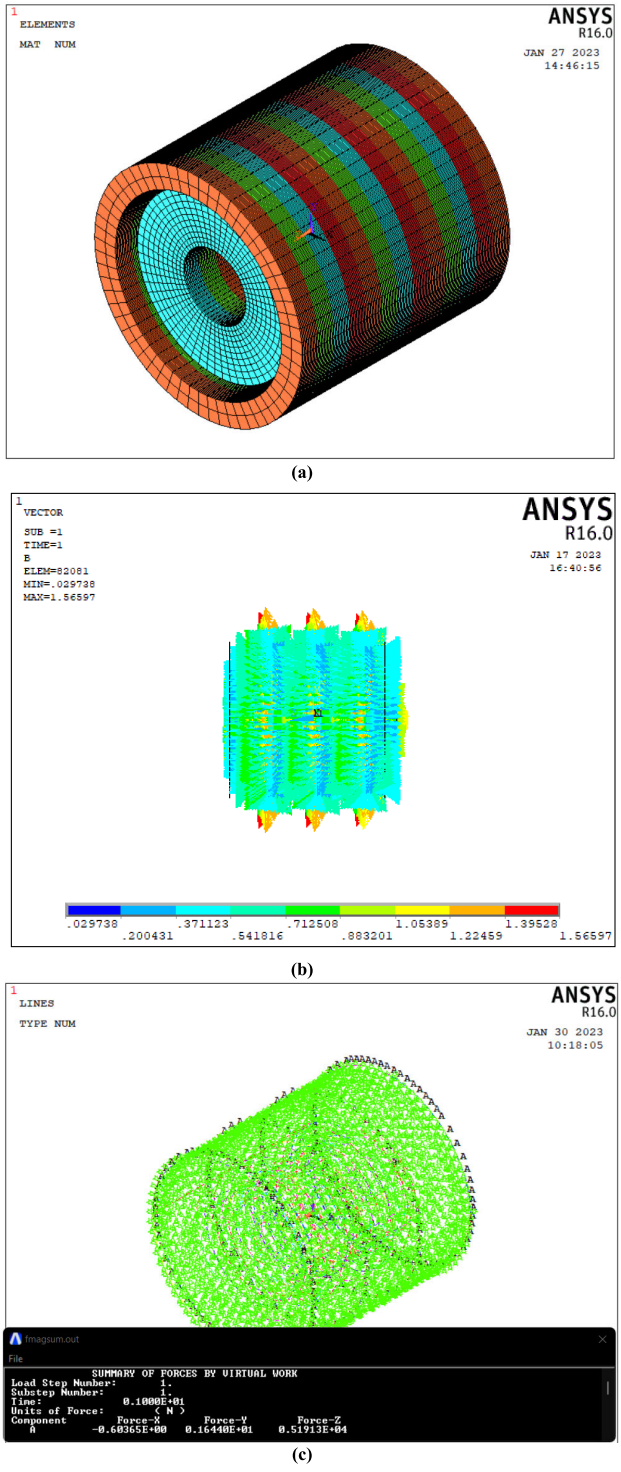

FIGURE 4. FEA results, (a) modeling of the stator as well as rotor rings, (b) flux lines generated in both rotor and stator, (c) Maximal axial force developed at an offset of z = 5.5 mm.

section. Table 4 shows the selected dimensions of the RMD thrust bearing with different air gaps and lengths so that the aspect ratio is varied from 0.25 to 1.5 in steps of 0.25. With the selected configuration, the optimal design parameters (Tables 5 and 6) are determined using corresponding

TABLE 4. Thrust bearing dimensions.

g(mm)	L (mm)	D4 (mm)	L/D4
0.5	20	80	0.25
	40		0.50
	60		0.75
	80		1.00
	100		1.25
	120		1.50
1.0	20		0.25
	40		0.50
	60		0.75
	80		1.00
	100		1.25
	120		1.50
1.5	20		0.25
	40		0.50
	60		0.75
	80		1.00
	100		1.25
	120		1.50
2.0	20		0.25
	40		0.50
	60		0.75
	80		1.00
	100		1.25
	120		1.50
2.5	20		0.25
	40		0.50
	60		0.75
	80		1.00
	100		1.25
	120		1.50
3	20		0.25
	40		0.50
	60		0.75
	80		1.00
	100		1.25
	120		1.50
3.5	20		0.25
	40		0.50
	60		0.75
	80		1.00
	100		1.25
	120		1.50
4	20		0.25
	40		0.50
	60		0.75
	80		1.00
	100		1.25
	120		1.50

curve-fit equations provided in Tables 1 and 2. The maximum force and stiffness are evaluated by using equations (1) - (7) for the optimized parameters concerning different aspect ratios considering optimum number of rings as well as only one ring in the control volume defining each aspect ratio. Then, the relationship between the ratios ((F_{zmax}/F_{zmaxs}) and (L/D4)), ((K_{zmax}/K_{zmaxs}) and (L/D4)) is established for different (g/D4) values and corresponding curve fit equations are shown in Figs. 5 and 6.

VI. APPLICATION EXAMPLE

In this section, the optimum design methodology for RMD thrust bearing is demonstrated with the help of an example. The steps involved in the selection and optimizing the bearing are given below.

1. For the optimization process, the specific values of L/D4 and g/D4 should be chosen.

TABLE 5. Optimized design parameters and the ratio of F_{zmax}/F_{zmaxs} for different g/D_4 and L/D_4 values.

g	D_4	g/D_4	L	L/D_4	g/D_4	H_{opt}/D_4	H_{opt}	n	n_{opt}	D_{1opt}/D_4	D1opt	D_{3opt}/D_4	D_{3opt}	F_{zmax}	(F_{zmaxs})	$\frac{F_{zmax}}{(F_{zmaxs})}$	R1	R2	R3	R4	L	n_{opt}
0.5	80	0.00625	20	0.25	0.00625	0.0523	4.184	4.78	5	0.328	26.24	0.8	64	2012.81	475.83	4.23	0.013	0.0315	0.032	0.04	0.02	5
			40	0.5	0.00625	0.0523	4.184	9.56	10	0.328	26.24	0.8	64	4544.18	452.91	10.03	0.013	0.0315	0.032	0.04	0.04	10
			60	0.75	0.00625	0.0523	4.184	14.34	14	0.328	26.24	0.8	64	6899.48	432.35	15.95	0.013	0.0315	0.032	0.04	0.06	14
			80	1	0.00625	0.0523	4.184	19.12	19	0.328	26.24	0.8	64	9453.01	422.85	22.35	0.013	0.0315	0.032	0.04	0.08	19
			100	1.25	0.00625	0.0523	4.184	23.90	24	0.328	26.24	0.8	64	11998.76	418.02	28.70	0.013	0.0315	0.032	0.04	0.1	24
			120	1.5	0.00625	0.0523	4.184	28.68	29	0.328	26.24	0.8	64	14540.32	415.38	35.00	0.013	0.0315	0.032	0.04	0.12	29
1	80	0.0125	20	0.25	0.0125	0.0568	4.544	4.40	4	0.315	25.2	0.8	64	1483.61	449.45	3.30	0.013	0.031	0.032	0.04	0.02	4
			40	0.5	0.0125	0.0568	4.544	8.80	9	0.315	25.2	0.8	64	3578.08	432.78	8.26	0.013	0.031	0.032	0.04	0.04	9
			60	0.75	0.0125	0.0568	4.544	13.20	13	0.315	25.2	0.8	64	5562.90	413.12	13.46	0.013	0.031	0.032	0.04	0.06	13
			80	1	0.0125	0.0568	4.544	17.60	18	0.315	25.2	0.8	64	7622.65	403.83	18.87	0.013	0.031	0.032	0.04	0.08	18
			100	1.25	0.0125	0.0568	4.544	22.00	22	0.315	25.2	0.8	64	9616.22	399.02	24.09	0.013	0.031	0.032	0.04	0.1	22
			120	1.5	0.0125	0.0568	4.544	26.40	26	0.315	25.2	0.8	64	11595.80	396.26	29.26	0.013	0.031	0.032	0.04	0.12	26
1.5	80	0.01875	20	0.25	0.01875	0.0633	5.064	3.94	4	0.307	24.56	0.8	64	1247.44	423.42	2.94	0.012	0.0305	0.032	0.04	0.02	4
			40	0.5	0.01875	0.0633	5.064	7.89	8	0.307	24.56	0.8	64	2902.62	412.10	7.04	0.012	0.0305	0.032	0.04	0.04	8
			60	0.75	0.01875	0.0633	5.064	11.84	12	0.307	24.56	0.8	64	4568.35	393.35	11.61	0.012	0.0305	0.032	0.04	0.06	12
			80	1	0.01875	0.0633	5.064	15.79	16	0.307	24.56	0.8	64	6234.03	384.31	16.22	0.012	0.0305	0.032	0.04	0.08	16
			100	1.25	0.01875	0.0633	5.064	19.74	20	0.307	24.56	0.8	64	7899.68	379.60	20.81	0.012	0.0305	0.032	0.04	0.1	20
			120	1.5	0.01875	0.0633	5.064	23.69	24	0.307	24.56	0.8	64	9565.30	376.90	25.37	0.012	0.0305	0.032	0.04	0.12	24
2	80	0.025	20	0.25	0.025	0.0706	5.648	3.54	4	0.302	24.16	0.8	64	1055.08	398.09	2.65	0.012	0.03	0.032	0.04	0.02	4
			40	0.5	0.025	0.0706	5.648	7.08	7	0.302	24.16	0.8	64	2391.25	391.44	6.10	0.012	0.03	0.032	0.04	0.04	7
			60	0.75	0.025	0.0706	5.648	10.62	11	0.302	24.16	0.8	64	3818.65	373.60	10.22	0.012	0.03	0.032	0.04	0.06	11
			80	1	0.025	0.0706	5.648	14.16	14	0.302	24.16	0.8	64	5182.13	364.84	14.20	0.012	0.03	0.032	0.04	0.08	14
			100	1.25	0.025	0.0706	5.648	17.70	18	0.302	24.16	0.8	64	6614.42	360.25	18.36	0.012	0.03	0.032	0.04	0.1	18
			120	1.5	0.025	0.0706	5.648	21.24	21	0.302	24.16	0.8	64	7973.03	357.61	22.29	0.012	0.03	0.032	0.04	0.12	21
2.5	80	0.03125	20	0.25	0.03125	0.0774	6.192	3.22	3	0.299	23.92	0.8	64	791.67	373.63	2.11	0.012	0.0295	0.032	0.04	0.02	3
			40	0.5	0.03125	0.0774	6.192	6.45	6	0.299	23.92	0.8	64	1970.67	371.09	5.31	0.012	0.0295	0.032	0.04	0.04	6
			60	0.75	0.03125	0.0774	6.192	9.6892	10	0.299	23.92	0.8	64	3239.09	354.14	9.14	0.012	0.0295	0.032	0.04	0.06	10
			80	1	0.03125	0.0774	6.192	12.91	13	0.299	23.92	0.8	64	4424.05	345.68	12.79	0.012	0.0295	0.032	0.04	0.08	13
			100	1.25	0.03125	0.0774	6.192	16.14	16	0.299	23.92	0.8	64	5603.52	341.22	16.42	0.012	0.0295	0.032	0.04	0.1	16
			120	1.5	0.03125	0.0774	6.192	19.37	19	0.299	23.92	0.8	64	6779.85	338.65	20.02	0.012	0.0295	0.032	0.04	0.12	19
3	80	0.0375	20	0.25	0.0375	0.0825	6.6	3.030303	3	0.298	23.84	0.8	64	695.44	350.00	1.98	0.01192	0.029	0.032	0.04	0.02	3
			40	0.5	0.0375	0.0825	6.6	6.060606	6	0.298	23.84	0.8	64	1735.13	351.03	4.94	0.01192	0.029	0.032	0.04	0.04	6
			60	0.75	0.0375	0.0825	6.6	9.090909	9	0.298	23.84	0.8	64	2776.13	334.96	8.28	0.01192	0.029	0.032	0.04	0.06	9
			80	1	0.0375	0.0825	6.6	12.12121	12	0.298	23.84	0.8	64	3817.63	326.81	11.68	0.01192	0.029	0.032	0.04	0.08	12
			100	1.25	0.0375	0.0825	6.6	15.15152	15	0.298	23.84	0.8	64	4859.28	322.50	15.06	0.01192	0.029	0.032	0.04	0.1	15
			120	1.5	0.0375	0.0825	6.6	18.18182	19	0.298	23.84	0.8	64	5928.93	320.00	18.52	0.01192	0.029	0.032	0.04	0.12	19
3.5	80	0.0438	20	0.25	0.0438	0.0848	6.784	2.948113	3	0.299	23.92	0.8	64	613.41	327.18	1.87	0.01196	0.0285	0.032	0.04	0.02	3
			40	0.5	0.0438	0.0848	6.784	5.896226	6	0.299	23.92	0.8	64	1533.19	331.23	4.62	0.01196	0.0285	0.032	0.04	0.04	6
			60	0.75	0.0438	0.0848	6.784	8.84434	9	0.299	23.92	0.8	64	2451.23	316.03	7.75	0.01196	0.0285	0.032	0.04	0.06	9
			80	1	0.0438	0.0848	6.784	11.79245	12	0.299	23.92	0.8	64	3369.73	308.20	10.93	0.01196	0.0285	0.032	0.04	0.08	12
			100	1.25	0.0438	0.0848	6.784	14.74057	15	0.299	23.92	0.8	64	4288.37	304.05	14.10	0.01196	0.0285	0.032	0.04	0.1	15
			120	1.5	0.0438	0.0848	6.784	17.68868	18	0.299	23.92	0.8	64	5206.90	301.63	17.26	0.01196	0.0285	0.032	0.04	0.12	18
4	80	0.05	20	0.25	0.05	0.0831	6.648	3.008424	3	0.3	24	0.8	64	592.49	304.07	1.94	0.01203	0.028	0.032	0.04	0.02	3
			40	0.5	0.05	0.0831	6.648	6.016847	6	0.3	24	0.8	64	1537.56	310.06	4.95	0.01203	0.028	0.032	0.04	0.04	6
			60	0.75	0.05	0.0831	6.648	9.025271	9	0.3	24	0.8	64	2468.41	295.72	8.34	0.01203	0.028	0.032	0.04	0.06	9
			80	1	0.05	0.0831	6.648	12.03369	12	0.3	24	0.8	64	3457.67	288.29	11.99	0.01203	0.028	0.032	0.04	0.08	12
			100	1.25	0.05	0.0831	6.648	15.04212	15	0.3	24	0.8	64	4251.08	284.34	14.95	0.01203	0.028	0.032	0.04	0.1	15
			120	1.5	0.05	0.0831	6.648	18.05054	18	0.3	24	0.8	64	5013.38	282.05	17.77	0.01203	0.028	0.032	0.04	0.12	18

2. Based on the values D4 and L concerning the application, g is calculated.
3. Curve fit correlations are used to calculate optimal design parameters and the ratios F_{zmax}/F_{zmaxs}, K_{zmax}/K_{zmaxs} (Refer to Tables 1 and 2 as well as Figures 4 and 5.).
4. Force and stiffness produced for a single-ring configuration F_{zmaxs} and K_{zmaxs} are calculated using equations (1) and (7).
5. Finally, F_{zmax} and K_{zmax} are calculated using the ratios calculated in step 3.

A. CASE STUDY 1

Rotation magnetized direction thrust bearing is designed and optimized for $g/D_4 = 0.025$ and $L/D_4 = 0.5$ for maximum axial force and stiffness. Utilizing the steps outlined in this section and by assuming g=2 mm, the optimal design parameters as well as force and stiffness are determined.

TABLE 6. Optimized design parameters and the ratio of K_{zmax}/K_{zmaxs} for different g/D_4 and L/D_4 values.

g	D_4	g/D_4	L	L/D_4	g/D_4	H_{opt}/D_4	H_{opt}	n	n_{opt}	D_{1opt}/D_4	D1o	D_{3opt}/D_4	D_{3opt}	K_{zmax}	(K_{zmaxs})	$\frac{K_{zmax}}{(K_{zmaxs})}$	R1	R2	R3	R4	L	n_{opt}
0.5	80	0.00625	20	0.25	0.00625	0.0196	1.568	12.75	13	0.45	36	0.825	66	2158200	172480	12.51	0.018	0.0325	0.033	0.04	0.02	13
			40	0.5	0.00625	0.0196	1.568	25.51	26	0.45	36	0.825	66	4422600	168376.86	26.26	0.018	0.0325	0.033	0.04	0.04	26
			60	0.75	0.00625	0.0196	1.568	38.26	38	0.45	36	0.825	66	6604800	166570.19	39.65	0.018	0.0325	0.033	0.04	0.06	38
			80	1	0.00625	0.0196	1.568	51.02	51	0.45	36	0.825	66	8870000	165675.92	53.53	0.018	0.0325	0.033	0.04	0.08	51
			100	1.25	0.00625	0.0196	1.568	63.77	64	0.45	36	0.825	66	11135000	165188.66	67.40	0.018	0.0325	0.033	0.04	0.1	64
			120	1.5	0.00625	0.0196	1.568	76.53	77	0.45	36	0.825	66	13400000	164907.36	81.25	0.018	0.0325	0.033	0.04	0.12	77
1	80	0.0125	20	0.25	0.0125	0.0276	2.208	9.05	9	0.45	36	0.825	66	1143800	129790.95	8.81	0.018	0.032	0.033	0.04	0.02	9
			40	0.5	0.0125	0.0276	2.208	18.11	18	0.45	36	0.825	66	2381500	126317.96	18.85	0.018	0.032	0.033	0.04	0.04	18
			60	0.75	0.0125	0.0276	2.208	27.17	27	0.45	36	0.825	66	3619200	124602.62	29.04	0.018	0.032	0.033	0.04	0.06	27
			80	1	0.0125	0.0276	2.208	36.23	36	0.45	36	0.825	66	4856900	123746.24	39.24	0.018	0.032	0.033	0.04	0.08	36
			100	1.25	0.0125	0.0276	2.208	45.28	45	0.45	36	0.825	66	6094600	123278.86	49.43	0.018	0.032	0.033	0.04	0.1	45
			120	1.5	0.0125	0.0276	2.208	54.34	54	0.45	36	0.825	66	7332300	123009.04	59.60	0.018	0.032	0.033	0.04	0.12	54
1.5	80	0.01875	20	0.25	0.01875	0.0347	2.776	7.20	7	0.45	36	0.825	66	725530	104338.33	6.9	0.018	0.0315	0.033	0.04	0.02	7
			40	0.5	0.01875	0.0347	2.776	14.40	14	0.45	36	0.825	66	1534900	101250.38	15.15	0.018	0.0315	0.033	0.04	0.04	14
			60	0.75	0.01875	0.0347	2.776	21.61	22	0.45	36	0.825	66	2390200	99624.74	23.99	0.018	0.0315	0.033	0.04	0.06	22
			80	1	0.01875	0.0347	2.776	28.81	29	0.45	36	0.825	66	3199900	98805.89	32.38	0.018	0.0315	0.033	0.04	0.08	29
			100	1.25	0.01875	0.0347	2.776	36.02	36	0.45	36	0.825	66	4009300	98358.22	40.76	0.018	0.0315	0.033	0.04	0.1	36
			120	1.5	0.01875	0.0347	2.776	43.22	43	0.45	36	0.825	66	4818700	98099.79	49.12	0.018	0.0315	0.033	0.04	0.12	43
2	80	0.025	20	0.25	0.025	0.0409	3.272	6.11	6	0.45	36	0.825	66	510970	86800.10	5.88	0.018	0.031	0.033	0.04	0.02	6
			40	0.5	0.025	0.0409	3.272	12.22	12	0.45	36	0.825	66	1094200	84076.20	13.01	0.018	0.031	0.033	0.04	0.04	12
			60	0.75	0.025	0.0409	3.272	18.33	18	0.45	36	0.825	66	1677400	82538.54	20.32	0.018	0.031	0.033	0.04	0.06	18
			80	1	0.025	0.0409	3.272	24.44	24	0.45	36	0.825	66	2260600	81756.83	27.65	0.018	0.031	0.033	0.04	0.08	24
			100	1.25	0.025	0.0409	3.272	30.56	31	0.45	36	0.825	66	2882200	81328.72	35.43	0.018	0.031	0.033	0.04	0.1	31
			120	1.5	0.025	0.0409	3.272	36.67	37	0.45	36	0.825	66	3465700	81081.56	42.74	0.018	0.031	0.033	0.04	0.12	37
2.5	80	0.03125	20	0.25	0.03125	0.0462	3.696	5.41	5	0.45	36	0.825	66	366090	73735.29	4.96	0.018	0.0305	0.033	0.04	0.02	5
			40	0.5	0.03125	0.0462	3.696	10.82	11	0.45	36	0.825	66	833130	71353.73	11.67	0.018	0.0305	0.033	0.04	0.04	11
			60	0.75	0.03125	0.0462	3.696	16.23	16	0.45	36	0.825	66	1264400	69902.24	18.08	0.018	0.0305	0.033	0.04	0.06	16
			80	1	0.03125	0.0462	3.696	21.64	22	0.45	36	0.825	66	1727900	69157.28	24.98	0.018	0.0305	0.033	0.04	0.08	22
			100	1.25	0.03125	0.0462	3.696	27.05	27	0.45	36	0.825	66	2160100	68748.53	31.42	0.018	0.0305	0.033	0.04	0.1	27
			120	1.5	0.03125	0.0462	3.696	32.46	32	0.45	36	0.825	66	2591500	68512.56	37.82	0.018	0.0305	0.033	0.04	0.12	32
3	80	0.0375	20	0.25	0.0375	0.051	4.08	4.90	5	0.45	36	0.825	66	297813.8	63529.03	4.68	0.018	0.03	0.033	0.04	0.02	5
			40	0.5	0.0375	0.051	4.08	9.80	10	0.45	36	0.825	66	648769.30	61108.04	10.61	0.018	0.03	0.033	0.04	0.04	10
			60	0.75	0.0375	0.051	4.08	14.70	15	0.45	36	0.825	66	999979.46	59790.24	16.72	0.018	0.03	0.033	0.04	0.06	15
			80	1	0.0375	0.051	4.08	19.60	20	0.45	36	0.825	66	1351224.42	59208.57	22.82	0.018	0.03	0.033	0.04	0.08	20
			100	1.25	0.0375	0.051	4.08	24.50	25	0.45	36	0.825	66	1702479.85	58914.04	28.89	0.018	0.03	0.033	0.04	0.1	25
			120	1.5	0.0375	0.051	4.08	29.41	29	0.45	36	0.825	66	2028552.08	58746.81	34.53	0.018	0.03	0.033	0.04	0.12	29
3.5	80	0.0438	20	0.25	0.0438	0.0543	4.344	4.60	5	0.45	36	0.825	66	243637.24	55603.06	4.381	0.018	0.0295	0.033	0.04	0.02	5
			40	0.5	0.0438	0.0543	4.344	9.20	9	0.45	36	0.825	66	514261.42	53480.07	9.61	0.018	0.0295	0.033	0.04	0.04	9
			60	0.75	0.0438	0.0543	4.344	13.81	14	0.45	36	0.825	66	805280.11	52237.87	15.41	0.018	0.0295	0.033	0.04	0.06	14
			80	1	0.0438	0.0543	4.344	18.41	18	0.45	36	0.825	66	1076564.14	51684.55	20.82	0.018	0.0295	0.033	0.04	0.08	18
			100	1.25	0.0438	0.0543	4.344	23.02	23	0.45	36	0.825	66	1367588.03	51403.49	26.60	0.018	0.0295	0.033	0.04	0.1	23
			120	1.5	0.0438	0.0543	4.344	27.62	28	0.45	36	0.825	66	1657531.224	51243.68	32.34	0.018	0.0295	0.033	0.04	0.12	28
4	80	0.05	20	0.25	0.05	0.0558	4.464	4.48	4	0.426	34.13	0.825	66	179687.08	50011.72	3.59	0.017	0.029	0.033	0.04	0.02	4
			40	0.5	0.05	0.0558	4.464	8.96	9	0.426	34.13	0.825	66	419910.04	48300.04	8.69	0.017	0.029	0.033	0.04	0.04	9
			60	0.75	0.05	0.0558	4.464	13.44	13	0.426	34.13	0.825	66	643083.76	47085.18	13.65	0.017	0.029	0.033	0.04	0.06	13
			80	1	0.05	0.0558	4.464	17.92	18	0.426	34.13	0.825	66	879512.49	46528.15	18.90	0.017	0.029	0.033	0.04	0.08	18
			100	1.25	0.05	0.0558	4.464	22.40	22	0.426	34.13	0.825	66	1103528.09	46242.11	23.86	0.017	0.029	0.033	0.04	0.1	22
			120	1.5	0.05	0.0558	4.464	26.88	27	0.426	34.13	0.825	66	1339109.69	46078.60	29.06	0.017	0.029	0.033	0.04	0.12	27

The calculated values for maximum axial force, as well as stiffness and the corresponding optimized design variables, are given in Tables 7 and 8. Apart from using the proposed optimization method, the values of the maximum force and stiffness are also calculated using the mathematical model and results are provided in Tables 7 and 8. The results obtained from optimization are in close agreement with the values calculated using the mathematical model. The deviation of 0.046% and 1.12% are observed in force and stiffness values with respect to mathematical model results. In addition, the maximum axial force is calculated by modeling the optimized configuration in ANSYS (Fig. 7) and the deviation of 6.29% is observed in the axial force value with respect to the results of the optimization.

B. CASE STUDY 2 (PROTOTYPE MODEL)

In our previous research efforts, we designed and developed an RMD thrust bearing, which was subsequently presented

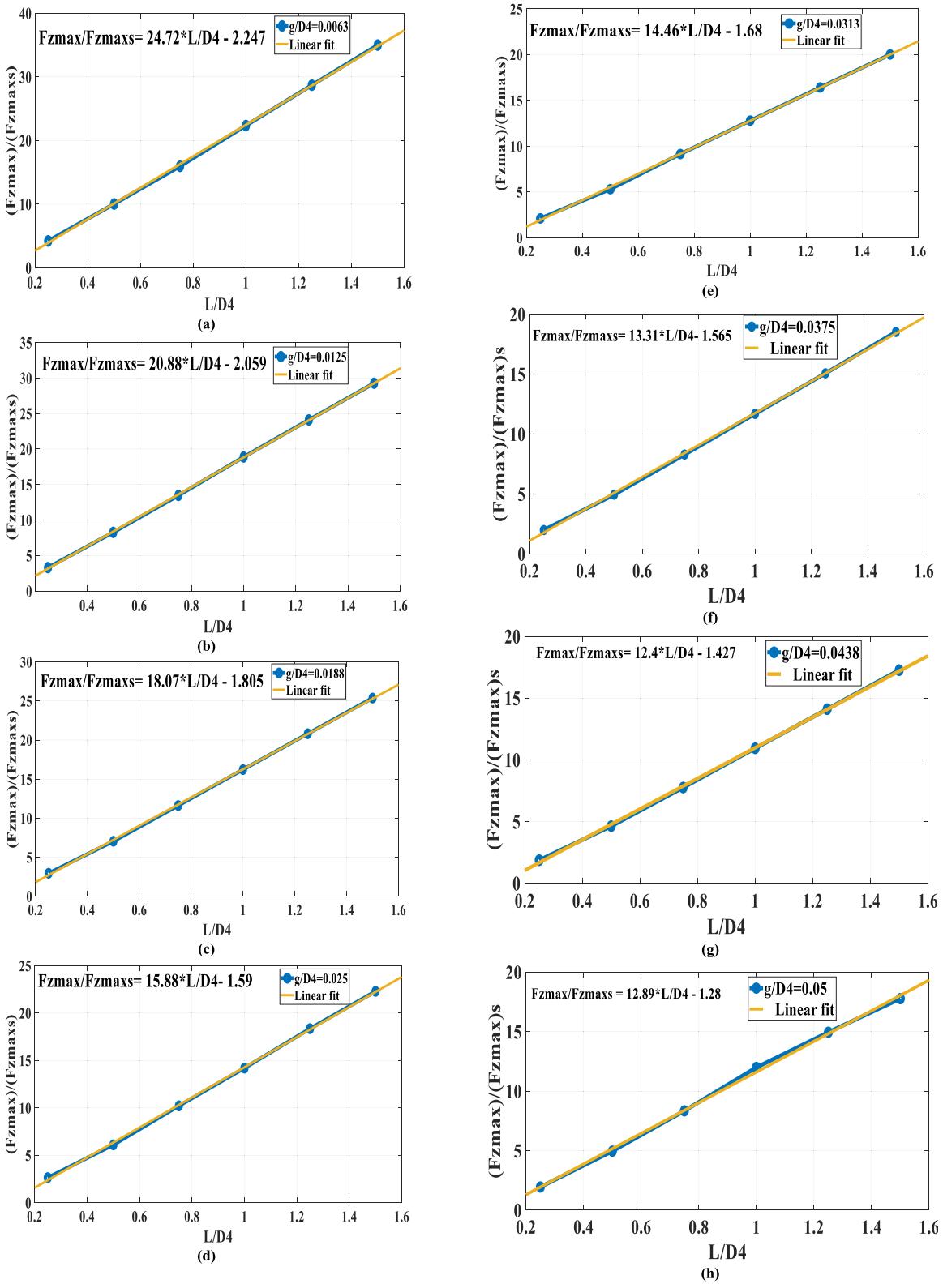

FIGURE 5. Relationship between F_{zmax}/F_{zmaxs} and L/D_4 for RMD thrust bearing with curve fit equations with g/D4 equals to (a) 0.00625, (b) 0.0125 (c) 0.01875 (d) 0.025 (e) 0.03125 (f) 0.0375 (g) 0.0438 (h) 0.05.

in [24]. The force and stiffness generated by the configured prototype were initially calculated using MATLAB code. To ensure the accuracy and reliability of these calculations, further verification was conducted using ANSYS simulations

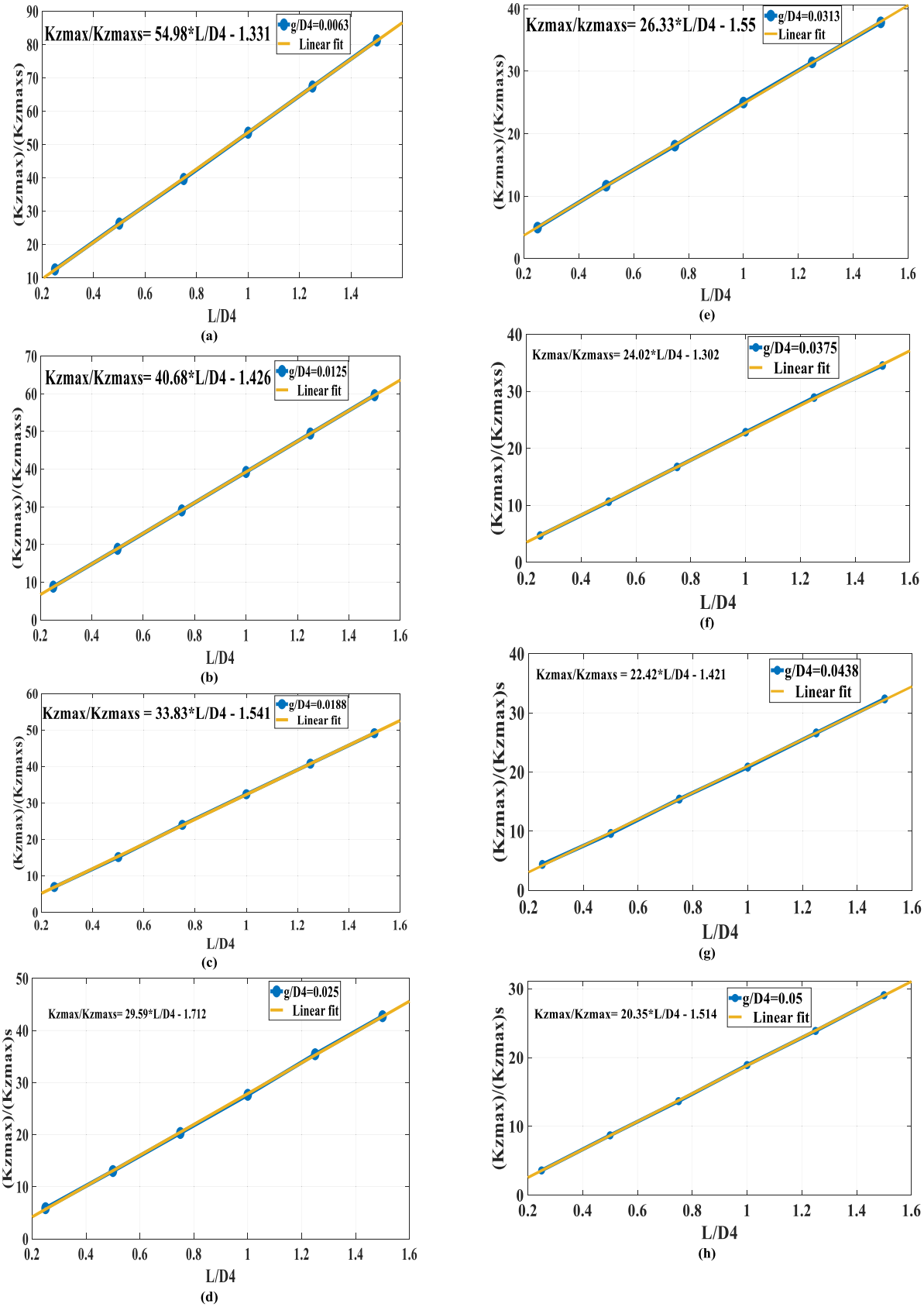

FIGURE 6. Relationship between K_{zmax}/K_{zmaxs} and L/D_4 for RMD thrust bearing with curve fit equations for g/D_4 equals to (a) 0.00625 (b) 0.0125 (c) 0.01875 (d) 0.025 (e) 0.03125 (f) 0.0375 (g) 0.0438 (h) 0.05.

TABLE 7. Results using the proposed optimization and mathematical model for F_{zmax}.

$g/D_4 = 0.025$ and $L/D_4 = 0.5$, assume g = 2mm, D_4 = 80mm L = 40mm		
Optimal Parameter	**Equations**	**Values of design variables**
n_{opt}	$\frac{H_o}{D_4} = -819 \times \left(\frac{g}{D_4}\right)^3 + 55.8 \times \left(\frac{g}{D_4}\right)^2 - 0.0957 \times \left(\frac{g}{D_4}\right) + 0.0509$	Ho = 5.648, $n_0 = 7$
D_{1opt}	$\left(\frac{D_1}{D_4}\right) = -517.2 \times \left(\frac{g}{D_4}\right)^3 + 74.11 \times \left(\frac{g}{D_4}\right)^2 - 3.326 \times \left(\frac{g}{D_4}\right) + 0.3464$	D_{10} = 24.16 mm
D_{3opt}	$\left(\frac{D_1}{D_4}\right) = 5.956 \times 10^{-15} \times \left(\frac{g}{D_4}\right) + 0.8$	D_{30} = 64 mm
D_{2opt}	D2 opt = D3 opt – 2g	D_{20} = 60 mm
$\frac{F_{zm}}{F_{zms}}$	$\frac{F_{zm}}{F_{zms}} = 15.881 \times \frac{L}{D_4} - 1.5896$	$\frac{F_{zm}}{F_{zms}}$ = 6.3509
F_{zms}	Using mathematical model for single ring	F_{zms} = 413.448 N
F_{zmo}	Calculation utilizing the proposed optimization method	F_{zmo} = 2621.68
F_{zm}	Calculation using mathematical model	F_{zm}=2621.25
F_{zmax}	FEA (ANSYS)	F_{zmax}=2786.6 N

TABLE 8. Results using the proposed optimization and mathematical model for K_{zmax}.

$g/D_4 = 0.025$ and $L/D_4 = 0.5$, assume g = 2mm, D_4 = 80mm L = 40mm		
Optimal Parameter	**Equations**	**Values of design variables**
n_{opt}	$\frac{H_o}{D_4} = -218.1 \times \left(\frac{g}{D_4}\right)^3 + 6.597 \times \left(\frac{g}{D_4}\right)^2 + 1.068 \times \left(\frac{g}{D_4}\right) + 0.01324$	Ho = 3.272, n_0 = 12
D_{1opt}		D_{10} = 36 mm
	$\left(\frac{D_1}{D_4}\right) = -2.913 \times 10^8 \times \left(\frac{g}{D_4}\right)^6 + 4.327 \times 10^7 \times \left(\frac{g}{D_4}\right)^5 - 2.529 \times 10^6 \times \left(\frac{g}{D_4}\right)^4 + 7.37 \times 10^4 \times \left(\frac{g}{D_4}\right)^3 - 1114 \times \left(\frac{g}{D_4}\right)^2 + 8.138 \times \left(\frac{g}{D_4}\right) + 0.4281$	
D_{3opt}	$\left(\frac{D_1}{D_4}\right) = 4.928 \times 10^{-15} \times \left(\frac{g}{D_4}\right) + 0.825$	D_{30} = 66 mm
D_{2opt}	D2 opt = D3 opt – 2g	D_{20} = 62 mm
$\frac{K_{zm}}{K_{zms}}$	$\frac{K_{zm}}{K_{zms}} = 29.587 \times \frac{L}{D_4} - 1.7124$	$\frac{K_{zm}}{K_{zms}}$= 13.0811
K_{zms}	Using mathematical model for single ring	K_{zms} = 82923.77 N/m
K_{zmo}	Calculation utilizing Proposed optimization method	K_{zmo} = 1081977.024 N/m
K_{zm}	Calculation using a Mathematical model	K_{zm} = 1094177.9407 N/m

and experimental testing. Illustration of the test rig is shown in Fig. 8. The dimensions of the developed configuration, as well as the corresponding force and stiffness values, are provided in Table 9.

Using the proposed optimization procedure, the developed RMD thrust bearing is optimized in a control volume pertaining to D4 = 68 mm and L = 15 mm and results are presented in Table 10. The results of the optimization are validated with mathematical model and FEA results (Fig. 9) The maximum axial force measured in the first prototype was 271.2 N. The maximum axial force increased to 325 N after implementing the proposed optimization procedure. Thus, in the optimized configuration the axial force generated is 19.92% higher than the original prototype. The value of the axial force for the optimized configuration obtained in ANSYS is 322.39 N which is very close to an optimized value of 325 N calculated using the proposed optimization method.

TABLE 9. The dimensions of RMD thrust bearing and characteristics.

Parameter	Values of design variables
n_1	H = 5, n_0 = 3
D_1	40
D_2	50
D_3	58
D_4	68
L	15
F_{zmax} (Mathematical model)	271.2 N
F_{zmax} (FEA)	269.75 N
F_{zmax} (Experimental)	241.32
K_{zmax}	93820 N

VII. MATLAB APP FOR DESIGN AND OPTIMIZATION

The proposed application is created in app Designer by considering two windows: procedure and RMD thrust bearing optimization. In the initial window (Fig. 10), a description of managing the framework used for the design, and optimization is provided.

In the second window, users can optimize the RMD thrust bearing by selecting various tabs such as input, g/D4, force calculation, and optimized results. An illustration of the RMD thrust bearing configuration is also provided for the user's

TABLE 10. Results of prototype using the proposed optimization procedure.

$g/D_4 = 0.05$ and $L/D_4 = 0.2$, assume g = 3.4mm, D_4 = 68mm L = 15mm		
Optimal Parameter	**Equations**	**Values of design variables**
n_{opt}	$\frac{H_o}{D_4} = -819 \times \left(\frac{g}{D_4}\right)^3 + 55.8 \times \left(\frac{g}{D_4}\right)^2 - 0.0957 \times \left(\frac{g}{D_4}\right) + 0.0509$	Ho = 5.66, $n_0 = 3$
D_{1opt}	$\left(\frac{D_1}{D_4}\right) = -517.2 \times \left(\frac{g}{D_4}\right)^3 + 74.11 \times \left(\frac{g}{D_4}\right)^2 - 3.326 \times \left(\frac{g}{D_4}\right) + 0.3464$	20.44 mm
D_{3opt}	$\left(\frac{D_1}{D_4}\right) = 5.956 \times 10^{-15} \times \left(\frac{g}{D_4}\right) + 0.8$	54.4 mm
D_{2opt}	D2 opt = D3 opt – 2g	47.6 mm
$\frac{F_{zm}}{F_{zms}}$	$\frac{F_{zm}}{F_{zms}} = 12.89 \times \frac{L}{D_4} - 1.28$	1.5558
F_{zms}	Using mathematical model for single ring	209 N
F_{zmo}	Calculation utilizing the proposed optimization method	325 N
F_{zmax}	FEA (ANSYS)	322.39 N

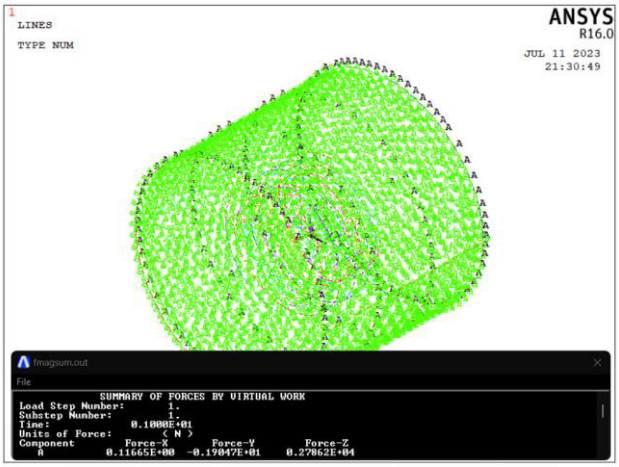

FIGURE 7. FEA results of the proposed optimization procedure.

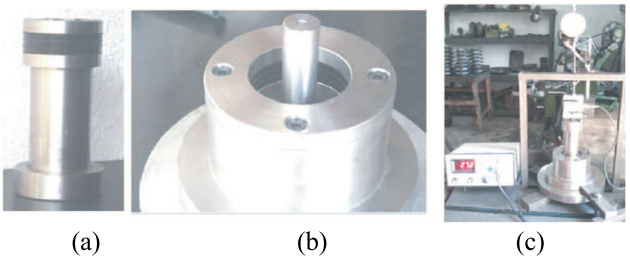

FIGURE 8. Description of the test rig used to measure axial force:(a) An illustrated representation is provided, showcasing the configuration of rings placed on the inner ring holder, also known as the rotor. (b) The positioning of the rings on the outer ring holder, referred to as the stator, is described. (c) A test rig is depicted, featuring both a load cell and a dial gauge, which are integral components used for measuring the axial force.

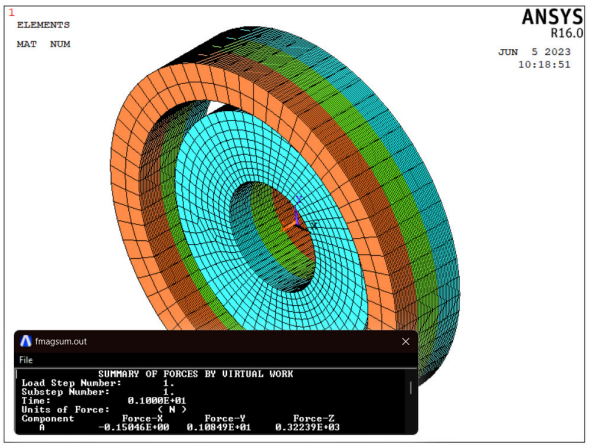

FIGURE 9. Modeling of rings in ANSYS along with value of F_{zmax}.

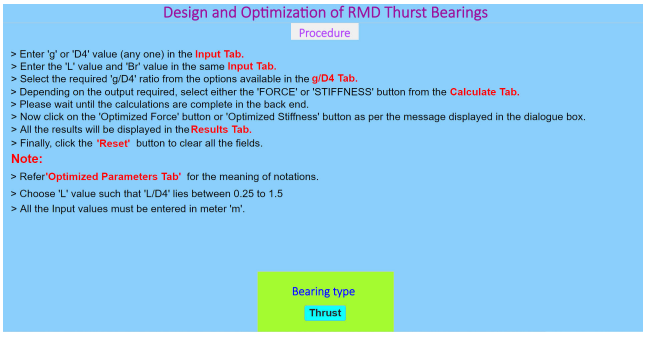

FIGURE 10. Initial procedure window of MATLAB app.

reference in Fig. 11. Four edit fields are available on the input tab: g, D_4, L, and Br.

The Fig. 11 shows how different values of L and D4 can be inputted into their respective fields, while different magnetic flux density (Br) values can be used. The users can enter their required L, D4 and Br values as per their requirements. The flowchart in Fig. 12 depicts the steps to be taken when using the MATLAB app.

In the proposed work, the optimization process is generalized by establishing the relationship between optimized parameters and air gap with respect to outer diameter. This generalization is with respect to geometrical aspects and it suits to permanent magnet with any magnetic flux density (Br) value. In addition, optimization is extended to different aspect ratios of the RMD configuration and the final maximized force and stiffness values of the optimized configuration are calculated by utilizing (running) the MATLAB code written for a single ring configuration in the selected control volume at the back end of the app.

The designer/user will be providing flux density value in the initial window of MATLAB app depending upon the selected magnet grade and thereafter all calculations will be carried out with respect to chosen magnetic flux density value.

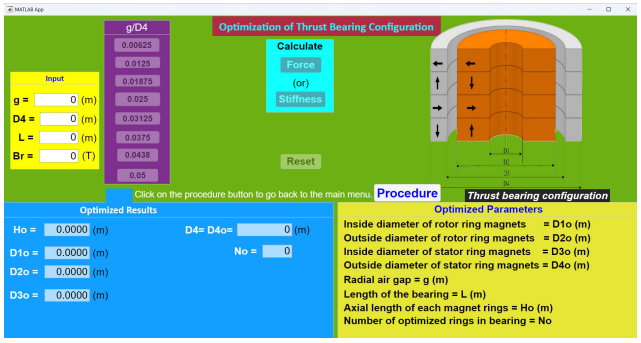

FIGURE 11. The second window of the MATLAB app for design and optimization.

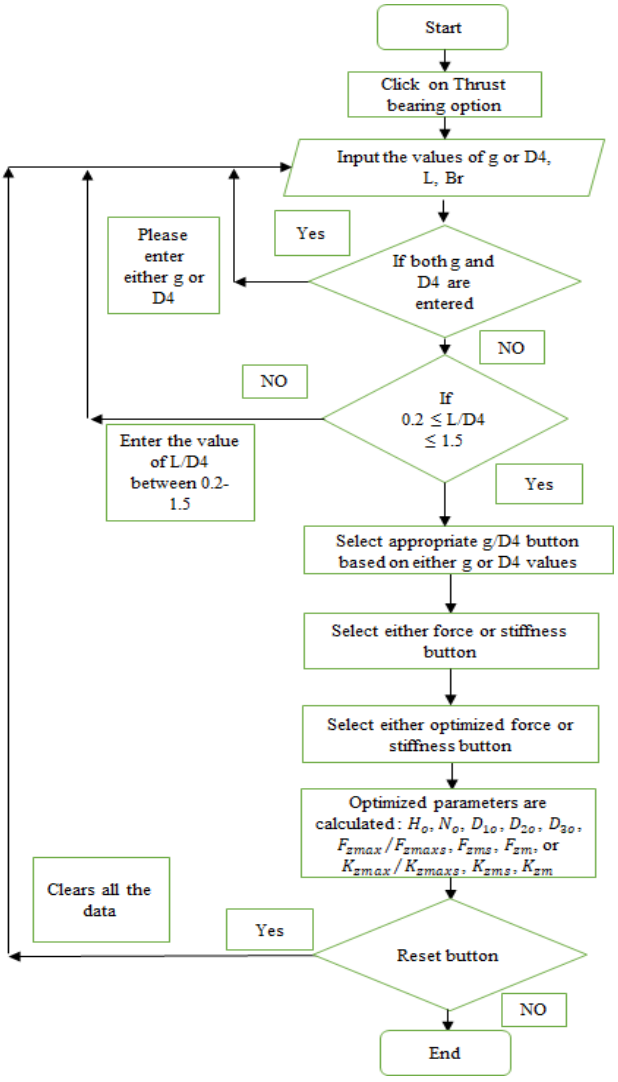

FIGURE 12. Flowchart depicting steps to be followed in MATLAB app.

VIII. RESULTS AND DISCUSSIONS

This section provides the usage of the MATLAB app developed to design and optimize RMD thrust PMB for different aspect ratios and any remanence values of the magnets.

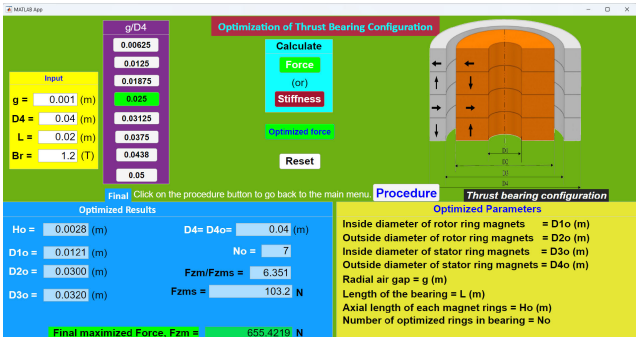

FIGURE 13. Optimized result for RMD thrust bearing for F_{zmax}.

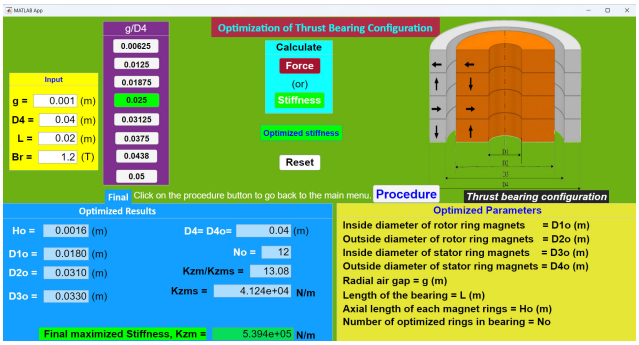

FIGURE 14. Optimized result for RMD thrust bearing for K_{zmax}.

A. EXAMPLE

For designing an optimized RMD thrust bearing for maximum force as well as stiffness, only D4 = 0.04 m, L = 0.02 m, $g/D_4 = 0.0025$, and Br = 1.2 T are chosen. By running the app, the optimized values of the design variables and maximized axial force for an RMD thrust bearing are shown in Fig. 13. The results obtained using app are in consistent with results presented in [30], and the deviation in the maximum axial forces is 4.79%. The maximum stiffness obtained for RMD thrust configuration is shown in Fig. 14. The value of maximum stiffness (5.88×10^5 N/m) obtained in [30] is in close agreement with value obtained using app (5.39×10^5N/m).

IX. CONCLUSION

In this paper, a complete generalized optimum design methodology and a computational framework (for selecting the optimum design parameters with maximized characteristics in a particular volume of the bearing) for RMD thrust bearing are presented. Based on the present work, the following conclusions are drawn:

- With the help of the proposed generalized optimization procedure, the optimal design parameters and corresponding maximized force and stiffness values of the RMD thrust bearing in a particular volume could be determined just by calculating the force and stiffness values of a monolithic bearing in that volume.

- Results of the proposed optimization procedure were validated using the results obtained by solving complicated 3D equations of force and stiffness for RMD thrust bearing. A deviation of 0.046% for maximum force and 1.12% for maximum stiffness was observed.
- To overcome the burden of calculating bearing features for a monolithic bearing using complicated equations in the proposed optimization method, a MATLAB computational framework was developed.
- A MATLAB app could be easily used to calculate optimal design parameters along with maximum bearing features in a particular volume just by providing values of L, $D4$, Br, and g.
- Results obtained using the MATLAB app were validated by selecting the case study of RMD thrust bearing from the literature.
- The proposed generalized optimization procedure and MATLAB app are best suited for an industrial use for any aspect ratio (L/D4) and magnetic flux density (Br) values.

REFERENCES

[1] E. H. Maslen and G. Schweitzer, *Magnetic Bearings*, vol. 53. Berlin, Germany: Springer, 2009, doi: 10.1007/978-3-642-00497-1.

[2] T. Ohji, S. Ichiyama, K. Amei, M. Sakui, and S. Yamada, "Conveyance test by oscillation and rotation to a permanent magnet repulsive-type conveyor," *IEEE Trans. Magn.*, vol. 40, no. 4, pp. 3057–3059, Jul. 2004, doi: 10.1109/TMAG.2004.832263.

[3] K. Jamari, "Radial forces analysis and rotational speed test of radial permanent magnetic bearing for horizontal axis wind turbine applications," in *Proc. AIP Conf.*, 2016, Art. no. 020034, doi: 10.1063/1.4945488.

[4] G. G. Sotelo, R. de Andrade, and A. C. Ferreira, "Magnetic bearing sets for a flywheel system," *IEEE Trans. Appl. Supercond.*, vol. 17, no. 2, pp. 2150–2153, Jun. 2007, doi: 10.1109/TASC.2007.899268.

[5] J. Fang, Y. Le, J. Sun, and K. Wang, "Analysis and design of passive magnetic bearing and damping system for high-speed compressor," *IEEE Trans. Magn.*, vol. 48, no. 9, pp. 2528–2537, Sep. 2012, doi: 10.1109/TMAG.2012.2196443.

[6] Y. Le, J. Fang, and J. Sun, "Design of a Halbach array permanent magnet damping system for high speed compressor with large thrust load," *IEEE Trans. Magn.*, vol. 51, no. 1, pp. 1–9, Jan. 2015, doi: 10.1109/TMAG.2014.2335715.

[7] S. I. Bekinal, S. S. Kulkarni, and S. Jana, "A hybrid (permanent magnet and foil) bearing set for complete passive levitation of high-speed rotors," *Proc. Inst. Mech. Eng., C, J. Mech. Eng. Sci.*, vol. 231, no. 20, pp. 3679–3689, Oct. 2017, doi: 10.1177/0954406216652647.

[8] S. I. Bekinal and M. Doddamani, "Friction-free permanent magnet bearings for rotating shafts: A comprehensive review," *Prog. Electromagn. Res. C*, vol. 104, pp. 171–186, 2020.

[9] S. C. Mukhopadhyay, T. Ohji, M. Iwahara, and S. Yamada, "Modeling and control of a new horizontal-shaft hybrid-type magnetic bearing," *IEEE Trans. Ind. Electron.*, vol. 47, no. 1, pp. 100–108, Feb. 2000.

[10] D. K. Supreeth, S. I. Bekinal, S. R. Chandranna, and M. Doddamani, "A review of superconducting magnetic bearings and their application," *IEEE Trans. Appl. Supercond.*, vol. 32, no. 3, pp. 1–15, Apr. 2022, doi: 10.1109/TASC.2022.3156813.

[11] W. Morales, R. Fusaro, and A. Kascak, "Permanent magnetic bearing for spacecraft applications," *Tribol. Trans.*, vol. 46, no. 3, pp. 460–464, Jan. 2003, doi: 10.1080/10402000308982651.

[12] J. Passenbrunner, G. Jungmayr, and W. Amrhein, "Design and analysis of a 1D actively stabilized system with viscoelastic damping support," *Actuators*, vol. 8, no. 2, pp. 1–18, 2019, doi: 10.3390/act8020033.

[13] D. Deshwal, S. I. Bekinal, and M. Doddamani, "Analysis of novel eddy current damper for multi-ring permanent magnet thrust bearing," *Prog. Electromagn. Res. M*, vol. 104, pp. 13–22, 2021, doi: 10.2528/PIERM21070107.

[14] J. G. Detoni, Q. Cui, N. Amati, and A. Tonoli, "Modeling and evaluation of damping coefficient of eddy current dampers in rotordynamic applications," *J. Sound Vib.*, vol. 373, pp. 52–65, Jul. 2016, doi: 10.1016/j.jsv.2016.03.013.

[15] S. I. Bekinal, T. R. Anil, and S. Jana, "Analysis of axially magnetized permanent magnet bearing characteristics," *Prog. Electromagn. Res. B*, vol. 44, pp. 327–343, 2012, doi: 10.2528/PIERB12080910.

[16] S. I. Bekinal, T. R. R. Anil, and S. Jana, "Analysis of radial magnetized permanent magnet bearing characteristics for five degrees of freedom," *Prog. Electromagn. Res. B*, vol. 52, pp. 307–326, 2013.

[17] S. I. Bekinal, T. R. R. Anil, and S. Jana, "Analysis of radial magnetized permanent magnet bearing characteristics," *Prog. Electromagn. Res. B*, vol. 47, pp. 87–105, 2013.

[18] B. Paden, N. Groom, and J. F. Antaki, "Design formulas for permanent-magnet bearings," *J. Mech. Des.*, vol. 125, no. 4, pp. 734–738, Dec. 2003, doi: 10.1115/1.1625402.

[19] Q. Tan, W. Li, and B. Liu, "Investigations on a permanent magnetic-hydrodynamic hybrid journal bearing," *Tribol. Int.*, vol. 35, no. 7, pp. 443–448, Jul. 2002, doi: 10.1016/S0301-679X(02)00026-9.

[20] P. Samanta and H. Hirani, "Magnetic bearing configurations: Theoretical and experimental studies," *IEEE Trans. Magn.*, vol. 44, no. 2, pp. 292–300, Feb. 2008, doi: 10.1109/TMAG.2007.912854.

[21] K. P. Lijesh and H. Hirani, "Modeling and development of RMD configuration magnetic bearing," *Tribol. Ind.*, vol. 37, no. 2, pp. 225–235, 2015.

[22] L. K. Parambil, "Design methodology for monolithic layer radial passive magnetic bearing," *Proc. Inst. Mech. Eng., J, J. Eng. Tribol.*, vol. 233, no. 6, pp. 992–1000, Jun. 2019, doi: 10.1177/1350650118806372.

[23] R. Ravaud, G. Lemarquand, and V. Lemarquand, "Halbach structures for permanent magnets bearings," *Prog. Electromagn. Res. M*, vol. 14, pp. 263–277, 2010, doi: 10.2528/PIERM10100401.

[24] S. I. Bekinal, T. R. R. Anil, S. Jana, S. S. Kulkarni, A. Sawant, N. Patil, and S. Dhond, "Permanent magnet thrust bearing: Theoretical and experimental results," *Prog. Electromagn. Res. B*, vol. 56, pp. 269–287, 2013.

[25] L.-L. Tian, X.-P. Ai, and Y.-Q. Tian, "Analytical model of magnetic force for axial stack permanent-magnet bearings," *IEEE Trans. Magn.*, vol. 48, no. 10, pp. 2592–2599, Oct. 2012, doi: 10.1109/TMAG.2012.2197635.

[26] S. I. Bekinal and S. Jana, "Generalized three-dimensional mathematical models for force and stiffness in axially, radially, and perpendicularly magnetized passive magnetic bearings with 'n' number of ring pairs," *J. Tribol.*, vol. 138, no. 3, pp. 1–9, Jul. 2016, doi: 10.1115/1.4032668.

[27] P. Samanta and H. Hirani, "A simplified optimization approach for permanent magnetic journal bearing," *Indian J. Tribol.*, vol. 2, no. 2, pp. 23–28, 2007.

[28] R. Moser, J. Sandtner, and H. Bleuler, "Optimization of repulsive passive magnetic bearings," *IEEE Trans. Magn.*, vol. 42, no. 8, pp. 2038–2042, Aug. 2006, doi: 10.1109/TMAG.2005.861160.

[29] S. I. Bekinal, M. Doddamani, and S. Jana, "Optimization of axially magnetized stack structured permanent magnet thrust bearing using three-dimensional mathematical model," *J. Tribol.*, vol. 139, no. 3, pp. 1–9, May 2017, doi: 10.1115/1.4034533.

[30] S. I. Bekinal, M. Doddamani, M. Vanarotti, and S. Jana, "Generalized optimization procedure for rotational magnetized direction permanent magnet thrust bearing configuration," *Proc. Inst. Mech. Eng., C, J. Mech. Eng. Sci.*, vol. 233, no. 7, pp. 2563–2573, Apr. 2019, doi: 10.1177/0954406218786976.

[31] S. I. Bekinal and M. Doddamani, "Optimum design methodology for axially polarized multi-ring radial and thrust permanent magnet bearings," *Prog. Electromagn. Res. B*, vol. 88, pp. 197–215, 2020, doi: 10.2528/pierb20090502.

[32] R. Kamath C, R. Bhat, S. I. Bekinal, T. S. Shetty, and M. Doddamani, "Design and optimization of multi-ring permanent magnet bearings for high-speed rotors—A computational framework," *Eng. Sci.*, vol. 10, pp. 194–202, Jan. 2021, doi: 10.30919/es8e536.

[33] A. Jalaik, S. D. Kumar, G. R. Chalageri, S. I. Bekinal, M. Doddamani, and S. R. Chandranna, "Damping system for an optimized rotation magnetized direction permanent magnet thrust bearing," *Prog. Electromagn. Res. C*, vol. 130, pp. 15–30, 2023, doi: 10.2528/PIERC22121404.

SUPREETH D. K. is currently a Research Scholar with the Department of Mechanical and Industrial Engineering, Manipal Institute of Technology, Manipal Academy of Higher Education (MAHE), Manipal, India. His research interest includes passive magnetic bearings and optimization.

SIDDAPPA I. BEKINAL is currently an Associate Professor with the Department of Mechanical and Industrial Engineering, Manipal Institute of Technology, Manipal Institute of Technology, Manipal Academy of Higher Education (MAHE), Manipal, India. His research interests include passive magnetic bearings, mechanical vibrations, rotor dynamics, turbomachinery, and mechanical vibrations energy harvesting.

SHIVAMURTHY R. C. is currently an Assistant Professor (Selection Grade) with the Department of Mechanical and Industrial Engineering, Manipal Institute of Technology, Manipal Institute of Technology, Manipal Academy of Higher Education (MAHE), Manipal, India. His research interests include surface engineering, tribology, metal matrix composites, 3D printing, metal processing, materials characterization, and failure analysis.

VIJAY G. S. is currently a Professor with the Department of Mechanical and Industrial Engineering, Manipal Institute of Technology, Manipal Academy of Higher Education (MAHE), Manipal, India. His research interests include bearing diagnostics, application of soft computing techniques to engineering and non-engineering domains, machinery vibration signal processing and analysis, finite element analysis, geometric modeling for cad, mechanical vibrations, fluid mechanics, operations research, and material science and metallurgy.

MRITYUNJAY DODDAMANI is currently an Associate Professor with the School of Mechanical and Materials Engineering, Indian Institute of Technology at Mandi, Mandi, Himachal Pradesh, India. His research interests include passive magnetic bearings, composite materials, additive manufacturing, and optimization techniques.